American Journal of VETERINARY RESEARCH
THE AMERICAN VETERINARY MEDICAL ASSOCIATION

Electrophysiologic evaluation of the phrenic nerve-diaphragm pathway in an intact, conscious calf model

Daniel J.-M. Desmecht, DVM; Annick S. Linden, DVM; Pierre M. Lekeux, DVM, PhD

Summary

Owing to technical and ethical limitations, a substantial part of the knowledge about the pathophysiologic mechanism of the human diaphragm has been obtained from studies in which phrenic nerve activation was usually carried out by direct surgical exposure of the nerves in the neck of deeply anesthetized, mechanically ventilated animals. Novel information has been gleaned from such studies, but the restrictive conditions under which it was collected preclude reliable extrapolation. We, therefore, addressed the question of whether accurate electrophysiologic evaluation of the phrenic nerve-diaphragm pathway can be performed in intact, nonanesthetized calves.

Transjugular phrenic activation was well tolerated, safe, specific, and able to achieve constant symmetric and supramaximal phrenic stimulations during prolonged periods. Eighteen noninvasive cutaneous and esophageal reception circuits were tested for their ability to record the diaphragmatic evoked potential. In addition, they were compared for specificity and reproducibility of the recorded potentials during prolonged periods of tidal or stimulated respiration. The best diaphragmatic potential was recorded from surface electrodes attached to the skin of the ninth and tenth intercostal spaces, using a xyphoidian reference.

We describe a method that allows easy, long-term, and reliable electrophysiologic evaluation of the phrenic nerve-diaphragm pathway in intact, conscious calves. It is hoped that such a model will produce relevant novel information regarding pathophysiology of the diaphragm.

Received for publication Feb 16, 1994.

From the Departments of Pathology (Desmecht), Bacteriology (Linden), and Physiology (Lekeux), Faculty of Veterinary Medicine, University of Liège, Boulevard de Colonster, Bât B43 Sart Tilman, B-4000 Liège, Belgium.

Supported by the Belgian Institut pour l'Encouragement de la Recherche Scientifique dans l'Industrie et l'Agriculture, IRSIA, grant No. 5475A, Brussels, Belgium.

The authors thank M. Leblond for technical assistance, P. Leroy for statistical analysis, and B. Collin for Figure 1.

Whether alteration in the force-generating capacity of the respiratory muscles attributable to lung disease,[1-5] or hypovolemic,[6] cardiogenic,[7] or septic[8] shock can result in life-threatening hypercapnic respiratory failure has been a controversial topic for nearly 60 years.[9-10] There still is no definitive answer to that question, mainly because investigations of the diaphragm involving physiopathology of ventilatory failure in human beings have been hampered by technical and ethical limitations. Moreover, a review of literature indicates that evaluations of diaphragm function in animal models were usually performed under the cover of some type and depth of general anesthesia, shortly after thoracotomy for electrode implantation, in animals that were usually mechanically ventilated and restrained in supine position. Novel information has been gleaned from those studies, but the restrictive conditions under which it was collected preclude reliable extrapolation and largely

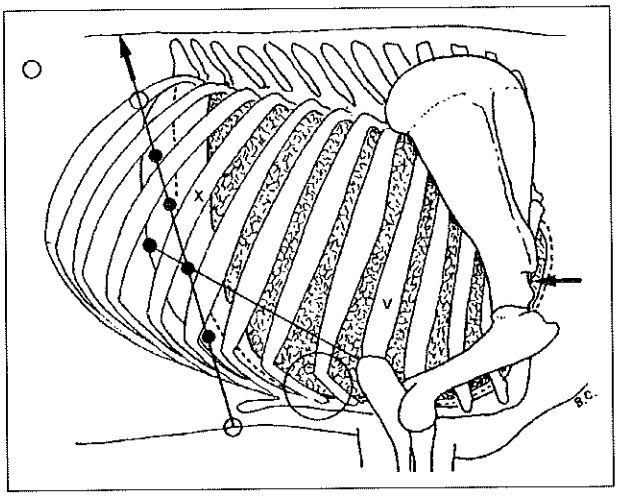

Figure 1—Electrode positions arbitrarily chosen for recording of body surface diaphragmatic compound action potentials. Diaphragmatic area of apposition on the inner thoracic wall extends from its costal insertions to the costodiaphragmatic recess of the pleurae. Closed rings = active electrodes and open rings = nonthoracic, 13th rib, and xyphoid process reference electrodes, respectively. Large circle = ground electrode, and arrow = estimated site of phrenic activation. V and X on ribs = fifth and tenth ribs, respectively. *See* text for further explanations.

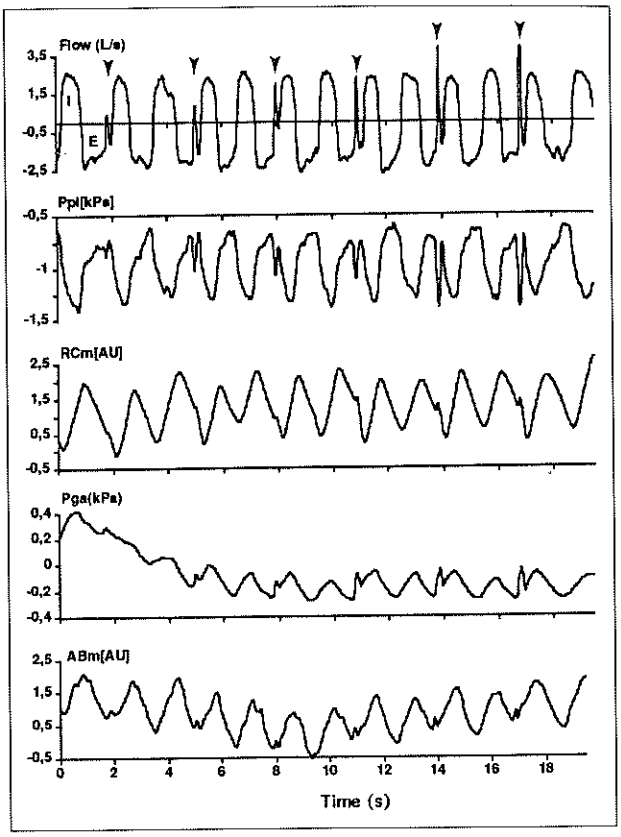

Figure 2—Typical thoraco-abdominal pressures and motions recorded while the stimulating probe is progressively advanced in the jugular vein. Notice that the probe can be easily brought in its right position, using visual monitoring of pressures. Arrows point to phrenic nerve stimulations. Ppl and Pga = pleural and gastric pressure, respectively. RCm and ABm = motion of the rib cage and the abdomen, respectively, an outward motion resulting in an upgoing waveform. AU = arbitrary unit, I = inspiration, and E = expiration.

contribute to the controversy. A method providing specific and reliable phrenic nerve-diaphragm functional parameters in intact, conscious animals is, therefore, crucially needed. Also, because respiratory diseases result in losses greater than all other diseases combined in the bovine species,[11] knowledge of the performances of the respiratory muscles in pneumonic calves would undoubtedly contribute to the understanding of the physiopathology and treatment of fatal respiratory failure.

Electrical phrenic nerve activation[12-17] provides a useful tool for detection of peripheral diaphragmatic weakness[18,19] and for assessment of drug effect on diaphragm function.[20] It is achieved directly after surgical isolation of the nerves in the neck,[13,15,17,21] transcutaneously,[14,16,18,22,23] transvenously,[12,24] or by use of needle electrodes.[25,26] There are, however, substantial limitations. Transcutaneous phrenic activation is painful because of the high voltage required to overcome resistance of the skin. Needle-induced phrenic activation, in turn, has potential hazards, such as pneumothorax, hemothorax, or nerve injury. In addition, maintaining a constant symmetric and maximal stimulus can often be problematic.[19,26] The transvenous approach supposedly requires a deep plane of anesthesia.[12,24] The primary purpose of the study reported here was to determine the most suitable method for activating the phrenic nerves in intact, nonanesthetized animals. Recording of the evoked potential also is necessary to ensure constant activation[27] or to estimate the neuromuscular coupling of the diaphragm.[28,29] Direct invasive surgical insertion of fishhook electrodes into the diaphragm allows reliable recording, but was documented to alter diaphragmatic function itself.[30] Use of gastroesophageal[28,29] or surface[27] electrodes, in turn, assumes that the electrical activity in the pickup volume of the electrodes (group of fibers the electrical activity of which is detected by the electrodes) fairly represents activity in each hemidiaphragm and that the recording conditions are unaffected by changes in lung volume or thoraco-abdominal configuration. This study was extended to determine the most suitable noninvasive reception circuit for capturing specific and reproducible evoked compound diaphragmatic action potentials.

An additional purpose of the study was to provide a method that would allow easy, reliable, long-term electrophysiologic evaluation of the phrenic nerve-diaphragm pathway in intact, conscious animals. Calves were chosen because of their wide use as experimental models of fatal lung diseases and endotoxemia. Such model could, therefore, produce information relevant to the pathophysiology of the diaphragm with regard to hypercapnic ventilatory failure.

Materials and Methods

Calves—Nine male Friesian calves were assigned to groups A and B, containing 3 and 6 animals, 48 ±

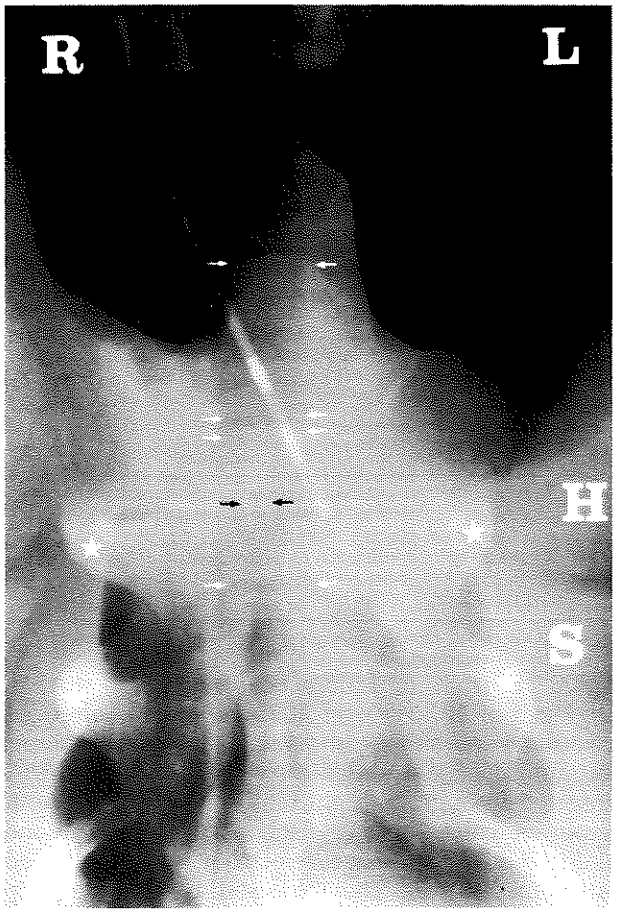

Figure 3—Ventrodorsal radiographic view of the cranial portion of the thorax, with the probe in place. Dark arrows surround the first obvious spinal process, which belongs to the first thoracic vertebra (T1). White arrows outline the seventh cervical vertebra and T1. Stars identify the first 2 pairs of ribs. H = humerus, S = scapula, R = right side, and L = left side. Notice that the 2 distal stimulating rings are located straight down from T1 vertebra.

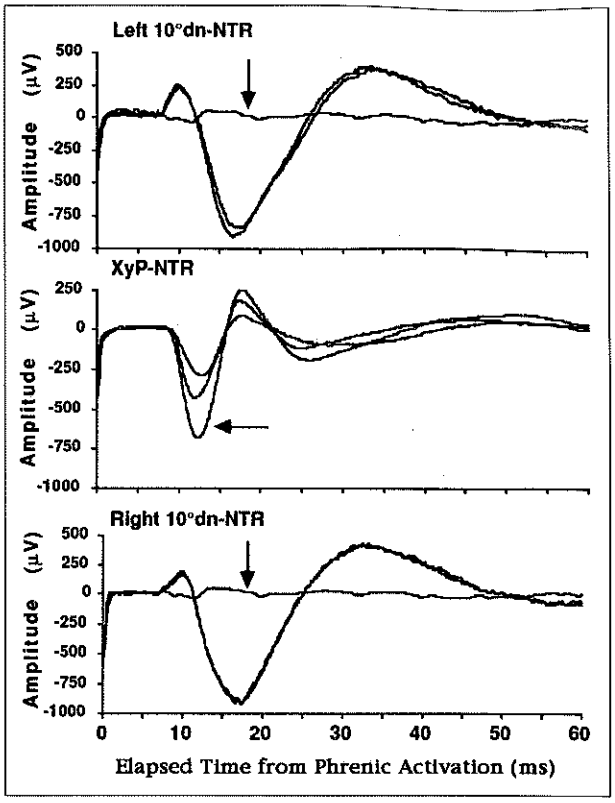

Figure 4—Diaphragmatic compound action potentials recorded in response to right unilateral, left unilateral, and bilateral phrenic activation, using 3 skin derivations. The NTR, XyP, and 10°dn represent electrodes placed over a nonthorax reference, the xyphoid process, and the down half of the tenth intercostal space, respectively. The recording circuits in these 3 and subsequent diagrams are denoted so that relative positivity at the first or negativity at the second electrode of the pair results in an upgoing waveform. Arrow identifies response to contralateral (top), bilateral (middle), and contralateral (bottom) phrenic activation. Notice that the 10°dn electrodes have an all or none kind of response, whereas activities roughly add at XyP and the polarities recorded at 10°dn and XyP evolve in contrasting fashion.

2 and 321 ± 11 days old (mean ± SD) and weighing 50 ± 1 and 304 ± 21 kg, respectively. One day before the study, fishhook (No. 10) electrodes were implanted in both hemidiaphragms of the 9 calves under xylazine[a]/gaiacolate[b]/thiopental[c]-induced and -maintained anesthesia. In group-A calves only, additional nickel-chrome 0.12-mm-diameter finewires,[d] bare of insulation for 2 to 3 mm, were sewn in the following muscles: interosseous—6th, 8th, and 10th outer and inner intercostals; intercartilagenous—6th, 8th, and 10th inner intercostals; and others—ventral scalenus, brachiocephalic, sternal triangular, ascending pectoral, and cutaneous trunci. Calves were determined to be free of respiratory tract and neurologic diseases on the basis of results of thorough clinical examination the day of the study. Neither anesthesia nor sedation was given. Gastric and esophageal balloons for gastric (Pga) and pleural (Ppl) pressure recordings[31] and abdominal (ABm) and thoracic (RCm) bands for thoracoabdominal wall motion recordings were inserted in calves.[32]

[a] Rompun Bayer, St Truiden, Belgium.
[b] Gujatal 10%, Aesculaap, Ghent, Belgium.
[c] Pentothal, Abott, Louvain-la-Neuve, Belgium.
[d] Microfil Industries, Renens-Lausanne, Switzerland.

Activation procedures—The calves were grounded via a lead plate glued on the skin of the right axillar fossa. In group-A calves, a lead plate anode was glued over the upper part of the sternal manubrium and a 12-gauge stainless steel needle, bare of Teflon insulation for 3 mm and serving as a cathode, was inserted horizontally through the fossa delimited by the descending and transverse pectoral and brachiocephalic muscles, protracted to the level of the first rib, then slightly withdrawn and moved inward and backward.

On the basis of anatomic planes,[33] it was hypothesized that the phrenic nerves could be activated through the venous walls. Accordingly, a 110-cm-long, 2-mm-diameter electrode catheter[e] equipped with 6 platinum electrodes separated by 10 mm was inserted in the right jugular vein through a percuta-

[e] Cardiac pacing lead TU 6/6F, Osypka GmbH, Grenzach-Wyhlen, Germany.

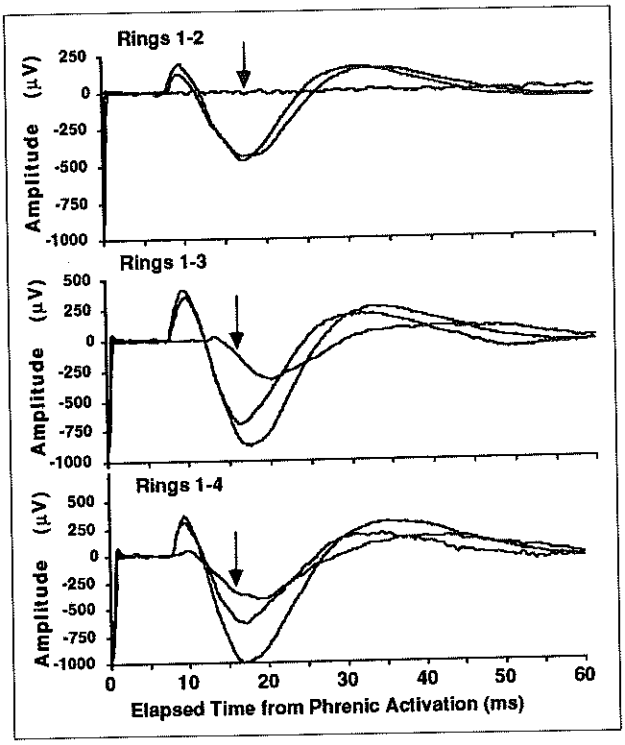

Figure 5—Diaphragmatic compound action potentials recorded in response to right unilateral, left unilateral, and bilateral phrenic activation, using 3 esophageal derivations. Rings 1, 2, 3, and 4 represent electrodes placed in the esophagus at the level of the cardia, and 4, 8, and 12 cm forward, respectively. Arrow identifies responses evoked by left unilateral phrenic activation. The largest responses were evoked by bilateral activation. Notice that the interelectrode distances greatly influence the recorded response, the left hemidiaphragm even being silent for the 1–2 pair.

neous sheath introducer placed in the mid-cervical area.[f] Immediately after insertion, single stimuli (rectangular pulses of 100- to 200-milliseconds duration, 10 to 20 V) were delivered via a pair of electrodes, using the proximal electrode as a cathode. Then the probe was gently advanced backward until twitches appeared on the Pga, Ppl, ABm, and RCm oscillograms. A mask-pneumotachograph assembly was then placed on the muzzle.[34] The airflow signal was integrated with respect to time to obtain tidal volume and was fed to an apparatus which, once activated, triggered all subsequent stimulations at end-expiratory zero airflow. Because we wanted to investigate the electrical event emanating from the diaphragm in response to single activation, which precedes in time any evoked mechanical action, we decided not to occlude the airway. Criteria and procedure for ensuring that the sequences of stimuli remained supramaximal were determined.

Reception procedures—The evoked compound hemidiaphragmatic action potentials (CDAP) were recorded from intramuscular (groups A and B), esophageal (group B), and surface (group B) electrodes, preamplified through a differential preamplifier (input resistance, 200 MΩ; common mode rejection ratio, 10,000:1), bandpass filtered between 20 and

[f] Desilet 8F, Vygon, Brussels, Belgium.

Table 1 — Comparison of the 2 respiratory patterns during which the stability of the recording conditions was studied

Characteristics	Unit	Eupnea	Hyperpnea
Timing			
Repiratory rate	min^{-1}	29 ± 3	42 ± 2
Inspiratory time	sec	0.98 ± 0.09	0.70 ± 0.02
Expiratory time	sec	1.14 ± 0.09	0.74 ± 0.02
Duty cycle	...	0.46 ± 0.01	0.49 ± 0.01
Flow			
Max inspiratory	L/s	2.69 ± 0.20	7.56 ± 0.38
Mean inspiratory	L/s	1.80 ± 0.79	6.08 ± 0.33
Max expiratory	L/s	2.55 ± 0.32	8.32 ± 0.42
Mean expiratory	L/s	1.57 ± 0.67	5.81 ± 0.33
Volume			
Tidal	L	1.74 ± 0.79	4.26 ± 0.16
Minute	L/min	50.28 ± 21.80	178.15 ± 9.58
Pressure			
pkIPpl	kPa	−1.45 ± 0.05	−2.12 ± 0.04
pkEPpl	kPa	−0.69 ± 0.05	−0.38 ± 0.05
maxΔPpl	kPa	0.75 ± 0.04	1.74 ± 0.05
Ppl_{EEZF}	kPa	−0.92 ± 0.05	−0.74 ± 0.04

pkIPpl = peak inspiratory pleural pressure; pkEPpl = peak expiratory pleural pressure; and maxΔPpl = peak-to-peak pleural pressure. Ppl_{EEZF} refers to the pleural pressure measured at end-expiratory zero flow, which gives an indirect estimation of lung volume and, hence, of diaphragm-to-electrodes spatial relation.
Values are means ± SD for 6 calves.

1,800 Hz (roll-off, 12dB/octave), amplified further, digitized at 10 kHz over 100 milliseconds after activation,[g] and stored on diskettes for later analysis. Intramuscular electrodes consisted of: 2 finewires[35] inserted through the right tenth intercostal space in group-A calves, and 2 fishhooks in group-A and group-B calves. Esophageal electrodes were also used in group-B calves. They consisted of 4 metal rings, 12 mm long, 6 mm in diameter, encircling a polyethylene catheter at distances of 1 (ring1), 4 (ring2), 7 (ring3), and 10 (ring4) cm proximal to a latex stabilizing balloon. The catheter was inserted through the nose until the balloon was in the stomach, then was inflated with 150 to 200 ml of air and gently withdrawn until a tug was felt. Surface electrodes consisted of 15 rectangular metal plates of about 8 × 4 mm, held to the shaved, scraped, and ethanol-cleansed skin by electrolyte paste[h] and further secured with glue.[i] Four electrodes were arbitrarily placed over each hemithorax in the eighth, ninth, tenth, and 11th intercostal spaces (hereafter denoted as 8, 9, 10up, and 11, respectively) on a line running from the xyphoid process (XyP) to the second lumbar vertebra, and a fifth one in the tenth intercostal space (hereafter denoted as 10dn) on a line running from the elbow to the electrode glued in the ninth intercostal space (Fig 1). The last 5 electrodes were glued on the XyP, the 13th intercostal space (R13), the back (B), the knee (K), and the toe (T).

As a convention, all reception circuits used in this paper were denoted so that relative positivity at the first electrode (active) or relative negativity at the second electrode (reference) would result in an upgoing waveform. Early in our preoperative assessments, we thought it essential to determine the degree to which an electrode used as reference was

[g] Superscope, GW Instruments, Somerville, Mass.
[h] EKGsol, Graphic Controls Ltd, Gananoque, Ontario, Canada.
[i] Bison, Perfecta Chemie, Goes, The Netherlands.

Table 2—Characteristics of hemidiaphragm action potentials recorded via 21 different reception circuits in 6 calves

Reception circuit	DL (ms)	D1 (ms)	D2 (ms)	D3 (ms)	A1 (μV)	A2 (μV)	A3 (μV)	S1 (μV·ms)	S2 (μV·ms)	S3 (μV·ms)
Skin										
8–NTR	7.0 ± 0.2 [ag]	3.4 ± 0.3 [aeh]	15.3 ± 0.5 [gik]	30.8 ± 0.9 [a]	335 ± 53 [a]	−411 ± 54 [ab]	211 ± 22 [agij]	1,494 ± 159 [bc]	3,649 ± 325 [ade]	3,489 ± 247 [ac]
9–NTR	7.2 ± 0.2 [abm]	3.5 ± 0.3 [ag]	13.9 ± 0.5 [hkp]	25.8 ± 0.9 [bc]	409 ± 53 [bfgj]	−883 ± 54 [cdfg]	347 ± 22 [be]	986 ± 159 [ak]	7,066 ± 325 [km]	4,834 ± 247 [bf]
10up–NTR	8.4 ± 0.2 [c]	0.0 ± 0.3 [b]	16.2 ± 0.5 [gj]	27.7 ± 0.9 [cek]	0 ± 53 [c]	−536 ± 54 [ahj]	259 ± 22 [dg]	0 ± 159 [ij]	4,570 ± 325 [bi]	3,950 ± 247 [cdg]
10dn–NTR	7.7 ± 0.2 [bdjk]	4.1 ± 0.3 [ad]	12.9 ± 0.5 [aejlnp]	22.9 ± 0.9 [fkl]	246 ± 53 [e]	−769 ± 54 [cdel]	328 ± 22 [bc]	688 ± 159 [aefh]	5,668 ± 325 [fj]	4,270 ± 247 [bd]
11–NTR	9.8 ± 0.2 [e]	2.0 ± 0.3 [cg]	13.7 ± 0.5 [hj]	26.7 ± 0.9 [cdk]	95 ± 53 [cd]	−664 ± 54 [eij]	331 ± 22 [bc]	277 ± 159 [defj]	5,124 ± 325 [cfi]	5,046 ± 247 [bf]
9–XyP	7.0 ± 0.2 [ag]	4.4 ± 0.3 [d]	12.5 ± 0.5 [adfj]	21.9 ± 0.9 [fh]	605 ± 53 [hk]	−1,070 ± 54 [k]	460 ± 22 [f]	1,687 ± 159 [c]	7,891 ± 325 [lm]	5,894 ± 247 [e]
10up–XyP	8.3 ± 0.2 [ch]	2.5 ± 0.3 [ceh]	15.5 ± 0.5 [gio]	26.5 ± 0.9 [bc]	251 ± 53 [e]	−688 ± 54 [il]	311 ± 22 [bd]	762 ± 159 [afh]	5,865 ± 325 [fj]	4,508 ± 247 [bg]
10dn–XyP	6.7 ± 0.2 [g]	4.1 ± 0.3 [ad]	12.1 ± 0.5 [defm]	23.0 ± 0.9 [fgk]	489 ± 53 [gh]	−1,011 ± 54 [fk]	468 ± 22 [f]	1,401 ± 159 [bc]	7,219 ± 325 [kl]	6,101 ± 247 [e]
11–XyP	7.9 ± 0.2 [fhl]	3.3 ± 0.3 [aeh]	12.4 ± 0.5 [fjl]	23.8 ± 0.9 [bf]	286 ± 53 [ef]	−842 ± 54 [cd]	402 ± 22 [e]	729 ± 159 [afh]	6,397 ± 325 [hjk]	5,438 ± 247 [ef]
8–10up	7.9 ± 0.2 [dfhk]	1.8 ± 0.3 [c]	13.9 ± 0.5 [chn]	25.3 ± 0.9 [bk]	−223 ± 53 [a]	−376 ± 54 [b]	49 ± 22 [h]	719 ± 159 [afh]	3,683 ± 325 [ade]	2,990 ± 247 [ajk]
8–11	7.8 ± 0.2 [dfhk]	1.9 ± 0.3 [c]	11.3 ± 0.5 [dfm]	18.6 ± 0.9 [j]	−277 ± 53 [a]	−370 ± 54 [b]	53 ± 22 [h]	953 ± 159 [ah]	3,609 ± 325 [ade]	2,410 ± 247 [iko]
9–11	7.2 ± 0.2 [aij]	3.0 ± 0.3 [efgi]	12.9 ± 0.5 [acefjp]	30.4 ± 0.9 [ae]	385 ± 53 [beg]	−852 ± 54 [d]	228 ± 22 [gj]	811 ± 159 [ah]	5,479 ± 325 [fg]	3,445 ± 247 [ac]
10dn–10up	7.6 ± 0.2 [bfil]	3.8 ± 0.3 [adf]	13.2 ± 0.5 [aehj]	22.8 ± 0.9 [fik]	342 ± 53 [be]	−784 ± 54 [degl]	317 ± 22 [bd]	901 ± 159 [ah]	5,911 ± 325 [fh]	4,196 ± 247 [dgh]
Esophagus										
ring1–NTR	8.1 ± 0.3 [cdf]	3.6 ± 0.5 [adeh]	10.5 ± 0.7 [bm]	21.2 ± 1.4 [fj]	266 ± 76 [dej]	−468 ± 78 [bh]	263 ± 32 [cdj]	243 ± 229 [dfj]	2,794 ± 468 [e]	2,842 ± 356 [ai]
ring1–XyP	7.9 ± 0.3 [cdf]	4.1 ± 0.5 [ad]	11.3 ± 0.7 [dlm]	21.2 ± 1.4 [fj]	494 ± 76 [bgk]	−610 ± 78 [chi]	304 ± 32 [bd]	1,093 ± 229 [ab]	3,961 ± 468 [abde]	3,445 ± 356 [ach]
ring1–ring2	7.3 ± 0.3 [adf]	3.6 ± 0.5 [adeh]	13.9 ± 0.7 [jkno]	21.2 ± 1.4 [fj]	311 ± 76 [beg]	−423 ± 78 [bh]	151 ± 32 [ai]	413 ± 229 [dghi]	3,131 ± 468 [ae]	1,551 ± 356 [lnp]
ring1–ring3	7.3 ± 0.3 [adfm]	4.1 ± 0.5 [ad]	14.9 ± 0.7 [gho]	24.1 ± 1.4 [bdfl]	467 ± 76 [bfghj]	−569 ± 78 [ahi]	157 ± 32 [ai]	876 ± 229 [ag]	4,311 ± 468 [abc]	1,701 ± 356 [mp]
ring1–ring4	8.1 ± 0.3 [ckl]	3.3 ± 0.5 [adehi]	17.0 ± 0.7 [i]	28.8 ± 1.4 [ac]	394 ± 76 [beg]	−538 ± 78 [bhi]	154 ± 32 [ai]	577 ± 229 [adj]	4,616 ± 468 [cdgi]	1,862 ± 356 [mno]
Muscle										
hook1–NTR	9.4 ± 0.3 [e]	2.6 ± 0.5 [cgh]	12.0 ± 0.7 [abdfj]	19.2 ± 1.4 [hj]	702 ± 76 [h]	−629 ± 78 [ehi]	241 ± 32 [dgj]	813 ± 229 [aefh]	3,991 ± 468 [abde]	2,165 ± 356 [ijlnp]
hook1–XyP	9.3 ± 0.3 [e]	2.7 ± 0.5 [cgh]	11.8 ± 0.7 [abdf]	20.2 ± 1.4 [ghijl]	743 ± 76 [h]	−596 ± 78 [aehi]	227 ± 32 [agij]	892 ± 229 [ah]	3,553 ± 468 [adei]	2,124 ± 356 [ilnp]
hook1–hook2	9.3 ± 0.3 [e]	2.2 ± 0.5 [ci]	12.5 ± 0.7 [acdfjp]	19.1 ± 1.4 [jk]	1,145 ± 76 [i]	−1,063 ± 78 [fk]	160 ± 32 [i]	1,427 ± 229 [bck]	3,443 ± 468 [ade]	1,358 ± 356 [lm]

Values are least-squares means (± SEM) of distal latency (DL); duration of first, second, and third phase (D1, D2, and D3, respectively); amplitude of first, second, and third phase (A1, A2, and A3, respectively); and area of first, second, and third phase (S1, S2, and S3, respectively) of evoked maximal compound hemidiaphragm action potentials recorded by 21 different reception circuits in 6 calves. NTR = nonthoracic reference; XyP = xyphoid process reference; 8, 9, 10, and 11 refer to the corresponding intercostal space; up = upper part of the intercostal space; and dn = down part of the intercostal space.

Only those values with different letters in brackets are significantly different ($P \leq 0.05$).

See text for further explanations.

recording the diaphragmatic response. Accordingly, recordings from reception circuits were obtained where the active electrode was gradually closer to the diaphragm: K–T, B–K, R13–B, XyP–B, ring1–B, ring2–B, ring3–B, and ring4–B. Afterward, simultaneous multiple[13] channel recordings were obtained from intramuscular, esophageal, and surface electrodes, using 21 arbitrary reception circuits to delineate distribution of the evoked CDAP and to determine the best circuit: hook1–hook2, hook1–B, hook1–XyP, ring1–ring2, ring1–ring3, ring1–ring4, ring1–B, ring1–XyP, 8–B, 9–B, 10up–B, 10dn–B, 11–B, 9–XyP, 10up–XyP, 10dn–XyP, 11–XyP, 8–10up, 8–11, 9–11, and 10dn–10up, the first 3 and the last 13 being repeated for right and left hemidiaphragms. Evoked CDAP from right and left hook1–hook2 circuits were recorded through channels 1 and 2. Care was taken to systematically associate intramuscular, esophageal, and surface reception systems in sets of simultaneous recordings through channels 3 to 6. The same was done for left and right hemidiaphragms.

Experimental design—The CDAP recorded by right and left hook1–hook2 circuits were recorded throughout the study, as a monitor of activation. Activation was considered maximal when a large increase in stimulus intensity did not result in further increase in the size of the CDAP. Stimuli were routinely delivered at twice the intensity required to cause maximal CDAP (on average, 80 V). In group-A calves, Pga, Ppl, ABm, and RCm tracings were obtained during needle and transvenous stimulations.

Seven series of 10 to 15 recordings were successively obtained from each calf in group B: 1 from K–T, B–K, R13–B, and XyP–B after uni- and bilateral activations, and 2–7 from the 37 circuits after right unilateral, left unilateral, or bilateral activations during eupnea and hyperpnea. Total evaluation time was approximately 8 hours. Type of activation (right unilateral, left unilateral, or bilateral) was achieved by adjusting the location of the probe in the vein, the stimulus voltage, and the interelectrode distance. The resting respiration (referred to here as eupnea) was varied by use of an expandable dead space that was adjusted to cause a stimulated inspired volume of about 250% of the tidal volume.

Data analysis—Ten CDAP were selected and averaged for each combination reception circuit-type of activation-breathing pattern. Time from activation to onset of first phase, or distal latency, peak amplitude, duration, and enclosed area were measured from the 2 or 3 phases of the remaining 1,332 mean maximal CDAP. Difference in a quantitative characteristic between eupnea and hyperpnea or left and right hemidiaphragms was expressed as percentage change relative to the measurements obtained for eupnea and the right hemidiaphragm, respectively. To examine reproducibility of the CDAP between the methods (intramuscular hooks, esophageal rings, and surface rectangles), hemidiaphragms (right and left), and patterns (eupnea and hyperpnea), a linear fixed model was fitted to the 10 CDAP variables recorded after bilateral activation[36] and was analyzed, using ANOVA.[37] The model included effect of animal, method, hemidiaphragm, pattern of breathing during which the measurements were made, interaction between method and pattern, and interaction between method and hemidiaphragm. To sharpen the analysis, the

method effect was divided into its own 21 levels and the between-reception circuits comparison of the captured CDAP was done by use of the same model, all pairs of least-square means being compared, using a *t*-test. The same kind of analysis was performed on the calculated percentage differences to define the impact of breathing strategy and hemidiaphragm on their repeatability. Finally, using the area of the depolarizing phase of CDAP evoked in response to right unilateral phrenic activation, factor analysis, using principal component strategy to extract the factors along with the orthotran/varimax transformation method, was performed, using the Pearson's correlation matrix computed for all possible pairs of reception circuits, the eighth intercostal space excluded.[38]

Results

Activation of phrenic nerves—Repeated needle stimulations allowed irregular, nonspecific unilateral phrenic activations during brief periods, the needle being rapidly displaced because of the movements of the punctured muscles. Along with these technical drawbacks, placement of the needle evoked signs of pain, was time consuming, and frequently caused hemorrhage and probably hemothorax.

Repeated transvenous stimulations required an approximately 15-minute period of adjustments before giving repeatable evidence of inspiration on the Pga, Ppl, ABm, RCm, and airflow tracings, suggesting that the diaphragm was activated (Fig 2). Unilateral and bilateral activations could be clinically individualized via the intensity of the inspiration and by monitoring the pressure tracings. Conclusive evidence was obtained from hook1–hook2-derived diaphragmatic electrograms, the amplitude of which closely paralleled pressure deflections and, at least in a narrow range (5 to 30 V), the stimulus voltage. Thoracic radiographic views taken with the probe in place confirmed preliminary dissections, the anode and cathode pair being exactly located vertically to the first thoracic vertebra (Fig 3). The long-term feasibility, safety, acceptability, and reliability of the technique for obtaining constant symmetric and maximal activation of the phrenic nerves was documented in calves of group B, which underwent, on average, 3 to 4 activations/min during 8 hours without manifesting excitement or cardiac arrhythmia. Moreover, the stimulus intensity for threshold activation remained constant between the first and the eighth hour. In all 9 calves, it was possible to adjust the probe to obtain stable right unilateral or bilateral activations without spread to the brachial plexus. Left unilateral activation, in turn, required frequent readjustments of the probe, the stimulation often becoming bilateral.

Electrograms for other muscles (group A) remained silent after activations, except for an occasional record from the right ascending pectoral muscle in 1 calf and systematic records from the right parasternal portion of the cutaneous trunci muscle in 2 calves.

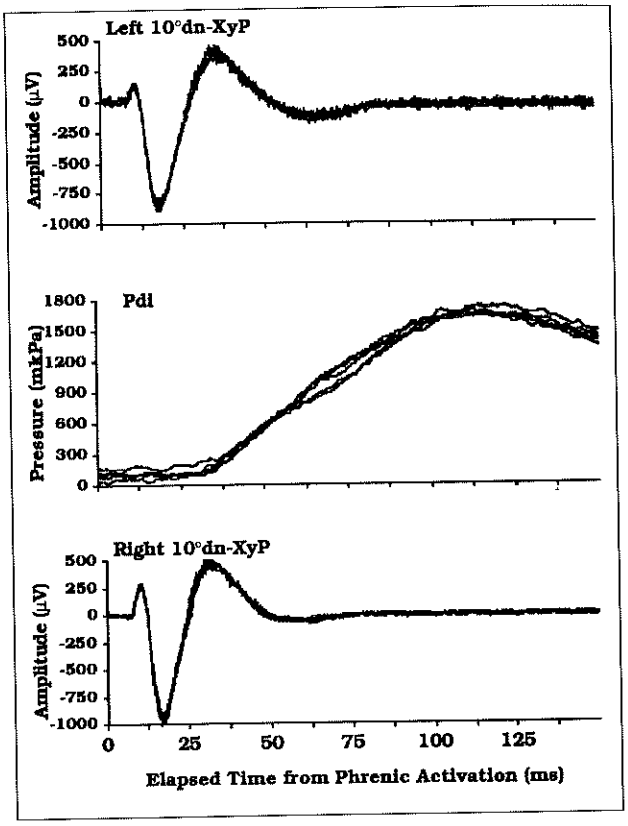

Figure 6—Diaphragmatic force and compound action potential evoked by bilateral phrenic activation (5 responses superimposed), using the best skin derivation. Pdi = transdiaphragmatic pressure; XyP = xyphoid process. Notice that the diaphragmatic potential precedes the mechanical response by 25 to 35 milliseconds.

Reception of Evoked Potentials

Assessment of referential recordings—Only nonthoracic electrodes (T, K, B) were indifferent to diaphragm contraction. Because of a better stability of the zero line, B was definitively chosen as the nonthoracic reference (NTR) for all unipolar circuits. The XyP–NTR recordings indicated biphasic responses with initial electronegativity that were of opposite polarity activity, compared with the activity captured by other unipolar circuits (Fig 4). Because of potential interest in the contribution of this out-of-phase opposite polarity activity, XyP was kept as a reference and xyphoidian bipolar circuits were also tested along with pure bipolar ones (hook-to-hook, ring-to-ring, and thorax-to-thorax). Ring1–NTR and ring2–NTR circuits captured a triphasic wave with initial positivity, whereas electrograms obtained from unipolar circuits, using rings 3 and 4 as active electrodes, had unique biphasic waves with initial positivity.

Qualitative assessment of electrograms—Obviously, repeatable CDAP could not be obtained during prolonged periods (1 hour) from fine wires inserted percutaneously in the diaphragm. Moreover, they were rapidly displaced by hyperpnea.

With each reference electrode (B, XyP, or hook2), electrograms obtained from intramuscular hooks were triphasic with initial electropositivity and a low-am-

plitude third phase. They had hypervariable morphology between individuals and were similar for ipsilateral and bilateral activations. Whatever the reference electrode (B, XyP, or ring 2, 3, or 4), electrograms obtained from esophageal rings after right unilateral and bilateral activation were similar, triphasic with initial electropositivity, and indicated comparable morphology between individuals. The CDAP recorded from ring1–XyP were systematically larger than those captured by ring1–NTR and were identical for right unilateral and bilateral activations. The ring1–NTR remained silent after left unilateral activation. The CDAP recorded from bipolar circuits after right unilateral activation first increased, then plateaued as the interelectrode distance was increased. After left activation, they were first absent then progressively increased. Bilateral activations generated CDAP that roughly corresponded to the electrical addition of both unilateral activations, whatever the bipolar montage (Fig 5). Electrograms obtained from surface reception circuits were identical for ipsilateral and bilateral activations, contralateral activations, in turn, never evoking any activity. The circuits including R8 as active site indicated irregular activities, with wide individual variations in morphology and amplitude. For each reference electrode, electrograms obtained from other surface electrodes, L8 included, roughly indicated a similar morphology between individuals and hemidiaphragms. Xyphoidian bipolar circuits always had larger waves than did unipolar and thorax-to-thorax circuits. The L8–NTR and L8–XyP CDAP were biphasic (50%) or triphasic with initial negativity or positivity, respectively, the depolarization phase having a rectangular aspect. The 9–NTR, 9–XyP, 10dn–NTR, and 10dn–XyP circuits were 100% triphasic with initial positivity; 9-NTR and 9–XyP had varied shoulders during repolarization; and 10dn–NTR and 10dn–XyP were the most regular and repeatable between individuals. The CDAP captured by 10up–NTR and 10up–XyP were 100% biphasic, regular, and repeatable between individuals, with initial electronegativity. The 11–NTR and 11–XyP CDAP were biphasic (50%) or triphasic, but of lower amplitude. The 4 thorax-to-thorax circuits gave repeatable CDAP between individuals, each circuit having its own characteristics: 100% biphasic, squared, and varied shoulders during depolarization and repolarization for circuit L8–L10up; 100% biphasic and regular for circuit L8–L11; 100% triphasic; larger for the left hemidiaphragm; and with long-lasting repolarization for circuits 9–11 and 10dn–10up. Obvious changes did not occur during hyperpnea for hook- and surface-derived potentials, except for some biphasic 10up–B and 10up–XyP CDAP which became triphasic. Conversely, the esophageal recordings had a systematic size reduction.

Quantitative assessment of electrograms—Objective description of the 2 breathing patterns during which CDAP were recorded was done (Table 1). Globally, most measurements of evoked CDAP were not significantly different between hemidiaphragms and patterns of breathing. To the contrary, the effect of the capturing method and the interaction between method and pattern were significant ($P \leq 0.05$). When the method effect was divided into 21 levels (ie, the reception circuits), the model confirmed a circuit effect ($P \leq 0.001$). The changes in size of the maximal CDAP recorded at the resting end expiratory level via 21 reception circuits were detailed (Table 2). Mean percentage changes between eupnea and hyperpnea were not significantly different between individuals and hemidiaphragms, but were highly dependent of the reception circuit ($P \leq 0.001$). Comparisons between pairs of mean changes indicated that hyperpnea was systematically associated with smaller esophageal CDAP, whereas intramuscular and surface CDAP were unaltered. Analysis of mean percentage differences between surface CDAP emanating from right and left hemidiaphragms revealed unequivocal influence of the reception circuit ($P \leq 0.001$), the left hemidiaphragm usually having a larger potential. Three factors were isolated by factor analysis of the Pearson's correlation matrix built for the area enclosed by the depolarization phase. Correlations between surface, muscular, and esophageal reception circuits and the first, second, and third factor were high: 0.852 ± 0.048 (mean ± SD), 0.931 ± 0.032, and 0.916 ± 0.070, respectively. On the contrary, not surface (0.291 ± 0.266 and 0.221 ± 0.134), nor muscular (0.215 ± 0.191 and 0.153 ± 0.124), nor esophageal (0.215 ± 0.156 and 0.172 ± 0.123) CDAP correlated with factors 2–3, 1–3, and 1–2, respectively. Comparison between diaphragmatic evoked electrogram and barogram indicated that the CDAP preceded the force development by 25 to 35 milliseconds (Fig 6).

Discussion

Activation of phrenic nerves—We found that insertion and adjustment of a catheter fitted with distal electrodes in the jugular trunk for transvenous activation of the phrenic nerves was a feasible, rapid, painless, and well tolerated procedure even in nonanesthetized, unsedated calves. Reliability of the technique was documented by the 8-hour maintenance of supramaximal bilateral activation, notwithstanding probable slight movements of the electrode in the blood flux. Because the vagus nerve and the myocardium are located fairly close to the phrenic nerve at its site of stimulation in the neck,[33] we looked for possible cardiac side-effects. In 9 calves, not heart rate changes, nor ECG timing, nor morphologic abnormalities were apparent. However, in our 3 years' experience, ventricular fibrillation occurred in 2 calves (2%). These 2 accidents affected the first and third calves ever tested and were attributable to descent of the stimulating electrode pair in the right ventricle. This emphasizes the necessity of practice by the operator before harmlessness can be ensured.

Reception of evoked potentials—Objective estimation of neural propagation, neuromuscular transmission, and propagation of impulses along the muscle requires a method that reliably reflects the total ef-

ferent activity of motor axons in the phrenic nerve. Our approach has been to record electrograms originating from the diaphragm via surface and esophageal electrodes on the assumption that this activity parallels efferent activity in the phrenic nerve. Possible sources of error in this type of recording must be considered.

Artifact from movement of the thoracic wall or mediastinum attributable to the diaphragmatic twitch itself has been excluded by measuring the onset of the mechanical event and documenting that it is preceded by the electrical response recorded by surface or esophageal electrodes (Fig 6).

Artifact may also result from activation of other muscle groups by the stimulus. In the 9 calves tested, it usually was possible to limit excitation to the phrenic nerves alone by a careful placement of the stimulating electrode. When the probe was moved away from its best adjustment or when higher stimulus intensities were given, associated spread of excitation to other muscles was observed (on the basis of clinical inspection and specific electromyograms in group-A calves) and the typical triphasic regular and repeatable diaphragmatic surface CDAP was replaced by an irregular potential of longer latency and sometimes inverse polarity. Surface recordings from the eighth right intercostal space were occasionally contaminated with activity in ascending pectoral or cutaneous trunci muscles, explaining the wide between-individuals variability of the CDAP recorded and justifying our decision to exclude CDAP recorded by circuits, using the eighth intercostal space for further use and analysis. Sometimes these interfering activations were detected when the diaphragmatic electrograms and thoracoabdominal pressures remained silent, which suggests that evoked pressure recordings should not be altered by such occasional spread of activation.

Misinterpretation may result from lack or unsteady specificity of a recorded CDAP for right, left, or both hemidiaphragms. In this regard, the trend of CDAP recorded from esophageal bipolar circuits after bilateral activations to become larger as the interelectrode distance increases is questionable, because the potentials evoked by right and left unilateral activations do not follow the same evolution (Fig 5). A first point is that the bilateral potential appears to correspond to the simple electrical addition of the 2 unilateral potentials. From our assessment of referential recordings, it can be predicted that rings 1 and 2 were close to the potential generator, leading to partial cancellation of right hemidiaphragm activity when used together as active and reference electrodes, respectively. This was not the case for ring1–ring3 and ring1–ring4 reception circuits, explaining why larger potentials were obtained. However, this cancellation phenomenon alone cannot explain why electrograms recorded by the most distal bipolar circuit after left unilateral activations remained absolutely silent in all 9 calves. This observation, which confirms the result obtained from ring1–NTR, indicates that rings 1 and 2 were absolutely indifferent to left hemidiaphragm activation. In our opinion, this finding could be explained if one postulates that the motor innervation of the perihiatal part of the bovine diaphragmatic crus is supplied by the right phrenic nerve alone. This hypothesis should be seriously considered. This asymetric innervation might be the functional parallel of anatomists' observation that, in Ongulae, right and left diaphragmatic intermediate perihiatal crura seem macroscopically to originate in the right muscle.[33] Whatever happens in the distal part of the esophagus, typical CDAP were recorded from ring1–ring3 and ring1–ring4. From the aforementioned information, it is clear that ring1 functions here as indifferent electrode, the real polarity of these CDAP being opposite. This interpretation is further strengthened by the fact that unipolar electrograms derived from rings 3 and 4 revealed unique biphasic potentials with initial electropositivity. Right and left unilateral activations lead to triphasic and biphasic CDAP, respectively, indicating undoubtfully that there were 2 spatial relations between active electrodes (ring1 and ring 3–ring4, respectively) and the level of the motor point of the activated muscles. This argument further pleads for the hypothesis that the gastroesophageal electrodes were asymetrically surrounded by the 2 activated muscles. Recording CDAP specific for right or left hemidiaphragms is not possible using esophageal electrodes in calves. Moreover, both electrodes used in a reception circuit might be capturing intermediate, right, and left diaphragmatic crura to variable degrees. To obtain reliable recording conditions, it is essential to maximize the interelectrode distance and to ensure stable spatial relation not only between the active electrode, but also the electrode taken as reference, and the surrounding structures. In comparison, the absolute specificity of surface CDAP for the ipsilateral hemidiaphragm must be emphasized. However, are they emanating from the costal, crural, or both parts of the activated hemidiaphragms? Factor analysis neatly associates 9–NTR, 10up–NTR, 10dn–NTR, 11–NTR, 9–XyP, 10up–XyP, 10dn–XyP, 11–XyP, 9–11, and 10dn–10up with factor 1; hook1–NTR, hook1–XyP, and hook1–hook2 with factor 2; and ring1–NTR, ring1–XyP, ring1–ring2, ring1–ring3, and ring1–ring4 to factor 3, suggesting that the recorded CDAP emanate from 3 electrical generators. If one assumes that the pickup volume of intramuscular electrodes is limited to a few thousand muscular cells surrounding the inserted hook, it can be hypothesized that factors 1, 2, and 3 should correspond to a substantial portion of the costal part, a few thousand costal muscular cells, and a portion of the crural part, respectively.

The quantitative repeatability of CDAP between tidal and stimulated breathing constitutes a crucial technical requirement before implementing the model during lung disease. In this regard, validity of the respiratory challenge used must be evaluated in terms of increased flows, volumes, and pressures which are the main variables acting on the length, tension, volume, and geometry of the interposed structures (thoracic walls, lungs, mediastinum) between the potentials' generator (diaphragm) and receptors (electrodes). From comparisons between Table 1 and published respiratory functional values

for airway[39] or alveolar[40] lung diseases in the same species, it clearly appears that the hyperpnea in our calves represents an experimental prototype of extreme conditions in cases of bovine respiratory tract diseases. Results of this study unequivocally indicate that, when respiration is stimulated, the assumption that CDAP characteristics vary in direct proportion to the quality of action potentials generation, propagation, and spread in the muscle remains valid for intramuscular and surface potentials, but does not apply to esophageal derived electrograms. Indeed, single supramaximal stimuli to the phrenic nerve produced esophageal CDAP that systematically decreased in size as the breathing strategy was altered. A similar result was obtained in human subjects voluntarily altering their diaphragmatic length and position.[19,41-43] Regarding the diaphragm, hyperpnea was associated with fiber lengthening at the end of expiration and probably with modification in position and geometry. Indeed, from the increase of peak expiratory Ppl (Table 1), it may be deduced that there was an expiratory effort that probably led to a decreased end-expiratory lung volume, this being confirmed by increase in end-expiratory zero flow Ppl. Regarding electrical transmission, hyperpnea was, thus, associated with a different spatial relation between the electrically active diaphragm and the esophageal electrodes. Accordingly, several factors may have contributed to this hyperpnea-induced artifact. Relative change in the radial distance between the crural fibers and the active recording electrode or a variable contribution to the recorded potentials from the crus by potentials produced by more distant regions of the diaphragm may have contributed. The latter factor is of crucial importance because we found that movements of the electrodes at rest in the esophagus are accompanied by various degrees of recording the left crus. The degree to which the esophageal reference electrodes were recording an activity may also have influenced the recorded CDAP, but this is unlikely to be a major factor because comparable artifacts were observed, using unipolar circuits. The conductivity of the volume conductor around the electrodes as a result of interposition of the lung[44] may have changed. However, similar artifactual changes occurred when the active electrode was referenced to B or XyP. Finally, a change in the tone of the perihiatal region of the esophagus, which is responsible for the tendency of the distal portion of the esophagus to grip the catheter, may vary and, therefore, affect recording conditions. Because of these specificity and reproducibility problems, we conclude that use of esophageal electrodes to document electrophysiologic changes should be avoided. Artifactual changes in thoracic wall surface recordings of maximal CDAP never occurred with alterations in breathing pattern, the little variation being comparable to the one recorded for the hooks. As previously mentioned, activations were systematically triggered at the end of expiration (ie, when the diaphragm would be expected to maintain close apposition to the rib cage). Stable recording conditions achieved were, therefore, not surprising because hyperpnea was accompanied by forced expirations (vide supra) in which diaphragmatic apposition to the inner thoracic wall should be intensified. The only exception concerned the CDAP given by 10up–XyP, which systematically switched morphology from biphasic to triphasic when respiration was stimulated.

Our studies, using simultaneous multiple channel recordings, establish that the surface diaphragmatic potential is best recorded from the ipsilateral ninth and tenth intercostal spaces, the former position usually providing somewhat larger response. Because the active electrodes placed over the eighth and 11th intercostal spaces may be contaminated with motor responses of other thoracic muscles or resulted in morphologically different CDAP between individuals, respectively, we do not recommend these sites for recording. Among the 3 derivations we extensively used, thorax-to-thorax bipolar, thorax-to-back unipolar, and thorax-to-XyP bipolar circuits provided diaphragmatic responses of progressively higher amplitude, respectively. Summation of out-of-phase thoracic and XyP potentials should provide a larger potential in the thorax-to-XyP circuits than those recorded from the thorax and an indifferent reference (NTR). The latter circuits, in turn, avoid partial cancellation of activity between thoracic electrodes capturing each in-phase diaphragmatic activity to variable degrees. To maximize sensitivity, we, thus, recommend use of thorax-to-XyP derivations. Interestingly, the recordings from XyP and 10up are diphasic, whereas the ones from 9 and 10dn are triphasic. These differences in morphology must be interpreted via the volume conduction theory,[45] according to which, XyP and 10up sites are suggested to be in the vicinity of the source of the muscular response that corresponds to the junctional region of the contributing muscle bundles. Conversely, the initial positivity that characterizes most of the recorded CDAP suggests that their recording electrodes were distant from the source of the response. Another question is how to explain that 10up and XyP sites appeared to be in the vicinity of the diaphragm's source of activity, whereas the 10dn site does not. A possible explanation is the complex shape of the diaphragm and, probably, the complex pattern of terminal innervation over its costal, sternal, and lumbar portions. This could also be the reason why the critical location of the belly electrode, giving a potential associating minimal latency, maximal size, and simplest diphasic configuration, was not found. The amplitude of our CDAP also was considerably lower (0.3 to 1 mV), compared with the 4 to 20 mV recorded from the small muscles of the human hand. These differences are probably attributable to the fact that the diaphragmatic potential is a far-field potential recorded at a considerable distance from the active muscle, compared with the near-field activity recorded on the hand. Also, the electrical resistance of bovine skin must be considered. The 6 calves being approximately the same size, the extremely low variation between individuals in distal latencies (<3%) emphasizes the good activation and reception technical standardization obtained. The between-circuits variation of distal latency (6.7 to 9.8 mil-

liseconds) in turn reflects variations in nerve length and, hence, conduction time to the different portions of the diaphragm.

We conclude that transvenous activation of the phrenic nerves and recording of the evoked potential via surface electrodes glued over the thorax is an easy and painless method that can be used in nonanesthetized and unsedated calves. It provides reliable quantitative information on phrenic conduction, phrenicodiaphragmatic neurotransmission, and diaphragmatic propagation of action potentials. It is easy to standardize and is free from iatrogenic risks. Stable stimulating and recording conditions can be achieved during prolonged periods, including episodes of labored breathing comparable to that of lung diseases. In this way, and in combination with force measurements, we hope this model may produce information relevant to the pathophysiology of the diaphragm in general, its role in hypercapnic ventilatory failure, and a pharmacologic means of improving its contractility.

References

1. Begin P, Grassino A. Inspiratory muscle dysfunction and chronic hypercapnia in chronic obstructive pulmonary disease. *Am Rev Respir Dis* 1991;143:905–912.
2. Efthimiou J, Fleming J, Spiro SG. Sternomastoid muscle function and fatigue in breathless patient with severe respiratory disease. *Am Rev Respir Dis* 1987;136:1099–1105.
3. Martin JG, Shore SA, Engel LA. Mechanical load and inspiratory muscle action during induced asthma. *Am Rev Respir Dis* 1983;128:455–460.
4. Rochester DF. Respiratory muscle weakness, pattern of breathing and CO_2 retention in chronic obstructive pulmonary disease. *Am Rev Respir Dis* 1991;143:901–903.
5. Wheatley JR, Westscala SJ, Engel LA. The effect of hyperinflation on respiratory muscle work in acute induced asthma. *Eur Respir J* 1990;3:625–632.
6. De Vito EL, Roncoroni AJ. Diaphragmatic fatigue in hypovolemic shock. *Medicina (B Aires)* 1990;50:35–42.
7. Aubier M, Viires N, Syllie G, et al. Respiratory muscle contribution to lactic acidosis in low cardiac output. *Am Rev Respir Dis* 1982;126:648–652.
8. Boczkowski J, Dureuil B, Branger C. Effects of sepsis on diaphragmatic function in rats. *Am Rev Respir Dis* 1988;138:260–265.
9. Killick EM. Resistance to inspiration and its effect on respiration in man. *J Physiol (Lond)* 1935;49:162–172.
10. Macklem PT, Roussos C. Respiratory muscle fatigue: a cause of respiratory failure? *Clin Sci Mol Med* 1977;53:419–422.
11. Lillie LE. The bovine respiratory complex. *Can Vet J* 1974; 15:233–242.
12. Aldrich TK, Appel D. Diaphragm fatigue induced by inspiratory resistive loading in spontaneously breathing rabbits. *J Appl Physiol* 1985;59:1527–1532.
13. Aubier M, Viires N, Murciano D, et al. Effects and mechanism of action of terbutaline on diaphragmatic contractility and fatigue. *J Appl Physiol* 1984;56:922–929.
14. Delhez L. *Contribution électromyographique à l'étude de la mécanique respiratoire et du contrôle nerveux des mouvements respiratoires chez l'homme.* Liège, Belgium: Vaillant-Carmanne, 1974;180–181.
15. Howell S, Roussos C. Isoproterenol and aminophylline improve contractility of fatigued canine diaphragm. *Am Rev Respir Dis* 1984;129:118–124.
16. Pengelly MD, Alderson A, Milic-Emili J. Mechanics of the diaphragm. *J Appl Physiol* 1971;30:797–805.
17. Viires N, Aubier M, Murciano D, et al. Effects of aminophylline on diaphragmatic fatigue during acute respiratory failure. *Am Rev Respir Dis* 1984;129:396–401.
18. Aubier M, Farkas G, De Troyer A, et al. Detection of diaphragmatic fatigue in man by phrenic stimulation. *J Appl Physiol* 1981;50:538–544.
19. Bellemare F, Bigland-Ritchie B. Assessment of human diaphragmatic strength and activation using phrenic nerve stimulation. *Respir Physiol* 1964;58:263–277.
20. Aubier M, Roussos C. Pharmacotherapy. In: Roussos C, Macklem PT, eds. *The thorax.* New York: Marcel Dekker Inc, 1986; 1373–1405.
21. Oliven A, Supinski GS, Kelsen SG. Functional adaptation of the diaphragm to chronic hyperinflation in emphysematous hamsters. *J Appl Physiol* 1986;60:225–231.
22. Bellemare F, Bigland-Ritchie B. Central components of diaphragmatic fatigue assessed by phrenic nerve stimulation. *J Appl Physiol* 1987;62:1307–1316.
23. McKenzie DK, Gandevia SC. Phrenic conduction times and twitch pressures of the human diaphragm. *J Appl Physiol* 1985; 58:1496–1504.
24. Warner A, Sackner MA. Transvenous phrenic nerve stimulation in anesthetized dogs. *J Appl Physiol* 1973;34:489–494.
25. Aubier M, Murciano D, Lecocguic Y, et al. Bilateral phrenic stimulation: a simple technique to assess diaphragmatic fatigue in humans. *J Appl Physiol* 1986;58:58–64.
26. Geddes LA, Simmons A. Artificial respiration in the dog by percutaneous, bilateral, phrenic nerve stimulation. *Am J Emerg Med* 1991;9:527–529.
27. Smith J, Bellemare F. Effect of lung volume on in vivo contraction characteristics of human diaphragm. *J Appl Physiol* 1987;62:1893–1900.
28. Grassino A, Goldman MD, Mead J, et al. Mechanics of the human diaphragm during voluntary contractions: statics. *J Appl Physiol* 1978;44:829–839.
29. Lopata M, Onal E, Ginzburg AS. Respiratory muscle function during CO_2 rebreathing with inspiratory flow-resistive loading. *J Appl Physiol* 1983;54:475–482.
30. Ford GT, Whitelaw WA, Rosenal TW, et al. Diaphragm function after upper abdominal surgery in humans. *Am Rev Respir Dis* 1983;127:431–436.
31. Desmecht D, Rollin F, Lekeux P. Transdiaphragmatic pressure measurement in cattle: technical data. *Res Vet Sci* 1992;53: 148–153.
32. Abraham WM, Watson H, Schneider A, et al. Noninvasive ventilatory monitoring by respiratory inductive plethysmography in conscious sheep. *J Appl Physiol* 1981;51:1657–1661.
33. Barone R. Mediastin. In: Barone R, ed. *Anatomie comparée des mammifères domestiques.* Lyons, France: Tixier & Fils, 1976;814–818.
34. Lekeux P, Hajer R, Breukink HJ. Pulmonary function testing in calves: technical data. *Am J Vet Res* 1984;45:342–345.
35. Basmajian JV, Stecko G. A new bipolar electrode for electromyography. *J Appl Physiol* 1962;17:849.
36. Littell RC, Freund RT, Spector PC. Comparison of several means: analysis of variance. In: Lopes J, Shelton PR, eds. *SAS series in statistical applications. SAS system for linear models.* Cary, NC: SAS Institute Inc, 1991;59–104.
37. Searle SR. Comparison of means. In: Searle SR, ed. *Linear models.* New York: John Wiley & Sons, 1971;412–457.
38. Gorsuch R. Factor extraction using principal component analysis. In: Gorsuch R, ed. *Factor analysis.* Hillsdale, England: Lawrence Erlbaum, 1983;229–251.
39. Lekeux P, Hajer R, Boon JH, et al. Physiological effects of experimental verminous bronchitis in Friesian calves. *Can J Comp Med* 1985;49:205–207.
40. Lekeux P, Hajer R, van den Ingh TSGAM, et al. Pathophysiologic study of 3-methylindole-induced pulmonary toxicosis in immature cattle. *Am J Vet Res* 1985;46:1629–1631.
41. Agostoni EG, Torri G. Diaphragm contraction as a limiting factor to maximum expiration. *J Appl Physiol* 1962;17:427–428.
42. Gandevia SC, McKenzie DK. Activation of the human diaphragm during maximal static efforts. *J Physiol (Lond)* 1985;367: 45–56.
43. Gandevia SC, McKenzie DK. Human diaphragmatic EMG: changes with lung volume and posture during supramaximal phrenic stimulation. *J Appl Physiol* 1986;60:1420–1428.
44. Grassino AE, Whitelaw WA, Milic-Emili J. Influence of lung volume and electrode position on electromyography of the diaphragm. *J Appl Physiol* 1976;40:971–975.
45. Bishop GH, Gilson AS. Action potentials from skeletal muscle. *Am J Physiol* 1929;89:135–151.